

# Strain-induced changes in the electronic valence-band structure of a cubic CdS(100) film

David W. Niles\* and Hartmut Höchst

Synchrotron Radiation Center, University of Wisconsin-Madison, 3731 Schneider Drive, Stoughton, Wisconsin 53589

(Received 26 August 1991)

High-resolution angle-resolved synchrotron-radiation photoemission spectroscopy was used to determine valence-band splittings and energy-dispersion changes in a strained, cubic CdS film grown by molecular-beam epitaxy on GaAs(100). Reflection high-energy electron-diffraction patterns indicate that the biaxial in-plane surface strain is initially compressively strained by  $\epsilon \sim 3.1\%$ . With increasing film thickness the overlayer starts to relax, leveling off at  $\epsilon \sim 1.0\%$  for a 170-Å-thick film. From photoemission spectra taken along the normal to the (100) surface, we measured the strain-induced splitting and modification of the energy dispersion of the CdS electronic valence bands along the  $\Gamma X$  direction. A comparison of the experimentally determined valence-band structure of the strained CdS film is made with a calculation based on the empirical pseudopotential method. The experiment verifies our theoretical prediction that strain shifts the more strongly dispersive splitoff band by  $\Delta E \sim 0.34$  eV to higher binding energy, away from the upper valence band.

## I. INTRODUCTION

The capability of growing high-quality epitaxial films that are under considerable tensile or compressive strain gave rise to a generation of semiconductor materials with technological applications.<sup>1-3</sup> For epitaxial films of thickness below a certain critical thickness  $h_c$ , strain generated by growth on a slightly lattice-mismatched substrate can be utilized as an additional design parameter to fine tune the electronic properties in the epilayer. Strain lifts the degeneracy of the heavy- and light-hole bands at the  $\Gamma$  point and modifies the dispersion relation  $E(k)$  of the valence bands, thus effectively changing transition energies as well as carrier mobilities.

Many studies of strain-induced effects in semiconductor heterostructures are either concerned with the band-gap variation as a function of applied stress (e.g., splitting of the  $\Gamma$ -point energy levels)<sup>4-8</sup> or in the changes of the valence-band offsets in strained heterostructures.<sup>9-12</sup> Recently, Hwang *et al.* have performed an analysis of thin, strained films of  $\text{In}_{0.2}\text{Ga}_{0.8}\text{As}$  on GaAs, and GaAs on  $\text{In}_{0.2}\text{Ga}_{0.8}\text{As}$ , where they found discernible strain-induced changes in the dispersions of both the  $\Delta_1$  and the nearly degenerate  $\Delta_3$  and  $\Delta_4$  bands.<sup>13</sup>

The present paper reports on strain-induced modifications along the (100) direction in thin cubic CdS films grown by molecular-beam epitaxy (MBE). Bulk CdS normally exists in the wurtzite crystal structure, but thin films readily grow in the cubic phase if offered a structurally matching substrate such as the zinc-blende-type lattice of GaAs.<sup>14,15</sup> The lattice constants for cubic CdS and GaAs are 5.83 and 5.65 Å, giving a lattice mismatch of  $\epsilon = -3.1\%$  for the initial growth. In a previous study using reflection high-energy electron diffraction (RHEED) and Raman spectroscopy, we showed that the interface strain partially relaxes as the thickness of the CdS film increases.<sup>16,17</sup> Raman spectra indicated that the surface layer strain profile was mainly frozen in the bulk of the sample as it was grown. Ultimately, a 170-Å-thick CdS overlayer was coherently strained within the critical thickness

of  $h_c \sim 12$  Å and relaxed gradually to  $\epsilon = -1.1\%$  in the outermost CdS layers.

We use angle-resolved ultraviolet photoemission spectroscopy to determine the strain-induced changes in the  $\Gamma$ -point valence-band splittings and band dispersions in a  $\sim 1.1\%$  compressively strained CdS film. The experimentally determined valence-band dispersions are compared to an empirical pseudopotential method (EPM) calculation of unstrained and strained CdS(100).

## II. EXPERIMENT

The GaAs(100) substrates used in the present investigation were grown *ex situ* by MBE and capped with an As overlayer. After mounting the GaAs substrate in the CdS growth chamber, the As cap was removed by heating the substrate to  $\sim 600^\circ\text{C}$  until a characteristic  $(2 \times 4)$  RHEED pattern appeared. The same decapping technique was used earlier and resulted in surfaces with exceptionally high structural qualities. CdS films were grown from a single liquid nitrogen shrouded boron nitride effusion cell. During the film growth, the substrate temperature was  $\sim 250^\circ\text{C}$ . The deposition rate was determined by a calibrated quartz-crystal monitor and verified with quantitative photoemission spectroscopy by monitoring the attenuation of a substrate's core line intensities.<sup>18,19</sup>

Photoemission experiments were performed *in situ* at the University of Wisconsin's Synchrotron Radiation Center. A Seya-Namioka beamline was used to obtain monochromatic photons in the range  $h\nu = 9\text{--}32$  eV. Photoemission spectra were measured with a hemispherical electron analyzer within an acceptance cone of  $\pm 1^\circ$  around the sample normal. The finite angular acceptance causes an uncertainty in the electron momentum of  $\Delta k \sim 0.05 \text{ \AA}^{-1}$ , which corresponds to  $\sim 7\%$  of the width of the Brillouin zone along the  $\Gamma X$  direction. The total-energy resolution of the monochromator plus electron analyzer system, as measured by the half width of the

Fermi edge from a metallic sample, was  $\Delta E \sim 125$  meV. The energy resolution is nearly independent over the useful photon range since the resolution of the electron energy analyzer, not the monochromator, was the limiting factor.

### III. RESULTS AND DISCUSSION

Figure 1 shows a plot of the biaxial in-plane relaxation behavior for CdS(100) overlayer as a function of its thickness. From the changes in the lateral spacing  $d$  between the (0 $\bar{1}$ ) and (01) RHEED reflections, we determined the in-plane surface lattice constant  $a_{\parallel} = 2\pi/d$  of the epilayer. The strain shown in Fig. 1 was calculated from the digitized RHEED pattern using  $\epsilon_{\parallel} = (a_{\parallel}^{\text{CdS}} - a_{\parallel}^{\text{GaAs}})/a_{\parallel}^{\text{GaAs}}$ . Up to a critical thickness of  $h_c \sim 12$  Å, the overlayer grows coherently with the GaAs bulk lattice spacing. Above the critical thickness, the in-plane lattice constant  $a_{\parallel}$  relaxes to reach a final misfit of  $\epsilon_{\parallel} \sim -0.8\%$  at 170 Å coverage. Using Matthews and Blakeslee's mechanical-equilibrium model,<sup>18</sup> we calculate a critical film thickness of  $h_c \sim 35$  Å for CdS film supported on one side by GaAs substrate. In consideration of the limitations of the theoretical model as well as the uncertainties in our experimental procedure in determining the exact film thickness and onset of the lattice relaxation, we conclude that the equilibrium model describes the observed instability of strained CdS films reasonably well.

Raman spectra of the CdS film showed a highly broadened, asymmetrical phonon spectrum.<sup>17</sup> Line-shape simulations of the Raman spectrum indicated that the strain was not homogeneous throughout the film, but rather varied with thickness in nearly the same fashion as the profile determined by the RHEED experiment.

The important point to understand from Fig. 1 is that the strain does not relax to zero, but instead levels off at a constant value near  $\sim 1.1\%$ . Since the escape depth for electrons in a typical angle-resolved valence-band spectra are only of the order of several angstroms, the vast majority of electrons we measure emanate from the region of the

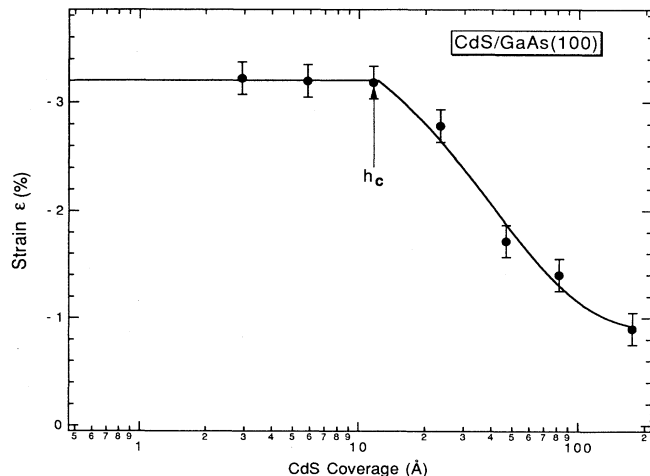


FIG. 1. Biaxial in-plane strain in a CdS overlayer grown on GaAs(100) as a function of thickness.

CdS film where the biaxial in-plane strain is nearly constant.

Applying the classical stress-strain theory, one may calculate the perpendicular lattice constant for a biaxially strained thin film of the cubic crystal. By forcing  $\epsilon_2 = \epsilon_3 = \epsilon_{\parallel}$ , classical theory would predict that  $\epsilon_{\perp} = -(2C_{12}/C_{11})\epsilon_{\parallel}$ , where  $C_{ij}$  are the elastic constants. Using the elastic coefficients for CdS ( $C_{11} = 7.8$  and  $C_{12} = 5.3 \times 10^{-11}$  dynes/cm<sup>2</sup>), the theoretical value for the perpendicular strain is  $\epsilon_{\perp} = 1.4\%$ . Note that this is not equivalent to applying a uniaxial stress in the (001) direction, where forcing  $\epsilon_2 = \epsilon_3 = \epsilon_{\parallel}$  yields  $\epsilon_{\parallel} = -\nu\epsilon_{\perp}$ . Poisson's ratio is given by  $\nu = -C_{12}/(C_{11} + C_{12})$ . We previously determined the average value of the perpendicular strain in the CdS film by x-ray diffraction and found  $\epsilon_{\perp} = 1.2\% \pm 0.2\%$ , which again indicates that elastic theory suffices to describe the strain behavior in cubic CdS films.<sup>18</sup>

It should be noted that a shortcoming of the simple elastic theory is expected for larger strains. Experiments with strained Si<sub>1-x</sub>Ge<sub>x</sub> alloys verify the prediction of the elastic model up to a value of  $\epsilon_{\perp} \sim 1.5\%$ . For the perpendicular lattice relaxation of thin films of Ge on Si(100) as well as for the growth of Si on Ge(100) where the in-plane strain is significantly higher than in the present CdS/GaAs interface, Chambers *et al.* found that the perpendicular lattice constant does not continue to relax as predicted by elastic theory.<sup>19</sup>

Figure 2 shows a selection of normal-emission valence-band photoemission spectra of a 170-Å-thick CdS(100) film. The features near the valence-band top labeled A

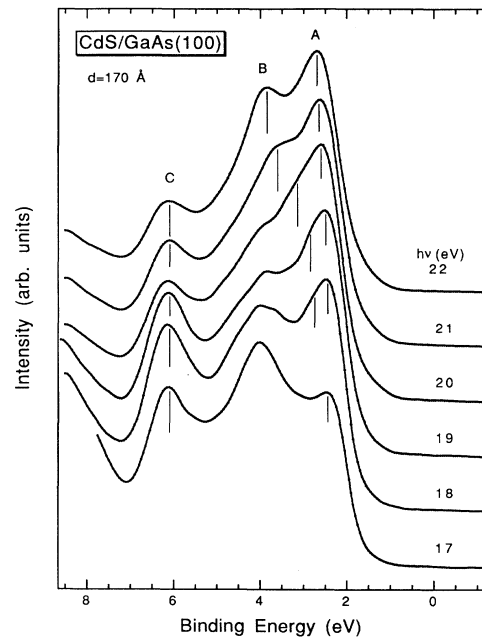


FIG. 2. Angle-resolved photoemission spectra from a 1% compressively strained CdS(100) film. The dispersive features labeled A and B are the results of a direct transition from the strain split valence bands. C is a nondispersive density-of-states feature around the region that was the  $X_6$  point in the unstrained film.

and *B*, which show strong dispersion effects with photon energy, are related to direct transitions from valence-band states. Two prominent nondispersive features are also visible in the spectra. The structure around 6 eV binding energy (labeled *C*) results from the high density of states region of the third valence band near the *X* point. The other nondispersive feature is centered at  $\sim 4$  eV in the  $h\nu=17$  eV spectra. Its intensity decreases rapidly with increasing photon energy. The origin is not certain at this point, and since that structure does not interfere with the analysis of the other dispersive structures, we have ignored it.

In order to determine the valence-band maximum, one can tune the incident photon energy until one observes the minimum binding energy associated with a direct transition from the top of the valence band.<sup>20</sup> For CdS, the minimum binding energy of the structure labeled *A* occurs for photons with  $h\nu=17$ –18 eV. At this point the valence-band maximum emission is strongest and centered 2.4 eV below the Fermi level. Increasing the photon energy leads to a downward dispersion of peak *A*, as the direct transition moves away from the  $\Gamma$  point. Peak *B* first appears for a slightly higher photon energy than peak *A*. The band labeled *B* also disperses downwards with increasing photon energy. We will describe in the next few paragraphs that this band results from the second valence band which has been strain split from *A*. Peak *B* merges into peak *C* for  $h\nu > 30$  eV; these spectra are not shown in Fig. 2.

While the binding energy *E* of an electron involved in an electronic transition can be inferred from the normal-emission valence-band spectra directly, the evaluation of the corresponding electron momentum **k** is not quite as straightforward. To determine the **k** vector for electronic transitions away from the  $\Gamma$  point, one must know the dispersion of either the final-state band or the initial valence band. For semiconductors, the final-state bands are successfully approximated over major parts of the Brillouin zone with free-electron bands of energy,

$$E = \frac{\hbar^2}{8\pi^2 m} (\mathbf{k} + \mathbf{G})^2 - U_0,$$

where **G** is a reciprocal-lattice vector and  $U_0$  is the inner potential.<sup>21</sup> In this equation, the zero of energy is taken to be the valence-band maximum. Note that the vacuum level does not appear in this equation, and since we have already determined the energy of the valence-band maximum with respect to the natural experimental zero (the Fermi level), the work function does not enter the equation either. The only variable parameter to be determined is the inner potential  $U_0$ .

We argued already that the direct transition at  $h\nu=17$  eV is from the valence-band maximum at  $k=0$ . To accomplish this, one must set  $U_0=3.9$  eV. This eliminates the remaining variable, and all the other *k* vectors associated with direct transitions are determined solely by their binding energies and the above equation. The experimentally determined  $E(\mathbf{k})$  values are plotted in Fig. 3.

The most remarkable result is a clear splitting of the triply degenerate valence-band maximum into two distinct components separated by  $\Delta E_s = 0.34 \pm 0.1$  eV. Strictly

speaking, the valence-band maximum in the absence of strain is already split by the spin-orbit interaction into a singlet and a doublet, but this splitting is only  $\Delta E_s \sim 0.07$  eV, which is below our energy resolution.<sup>22</sup> Away from the  $\Gamma$  point, the split-off band disperses more rapidly than the heavy-hole band, as is predicted in the case for unstrained CdS.

Also shown in Fig. 3 are the calculated valence-band structures for unstrained and 1.0% compressively strained CdS. We calculated the dispersions in both strained and unstrained CdS near the  $\Gamma$  point with the empirical pseudopotential method.<sup>23</sup> While the EPM method provides reasonably accurate energy splittings at the  $\Gamma$  point, the method is known to underestimate the total bandwidth. Taking this shortcoming of the calculation into account, we adjusted the calculated bandwidth to the experimentally determined width between the  $\Gamma$  point of the first band and the *X* point of the split-off second band, which is accurately determined by the nondispersive feature *C* at 3.7 eV below the top of the valence band. The calculated band dispersions are plotted as solid and dotted lines in Fig. 3. For the unstrained case, the valence-band maximum is essentially the triply degenerate  $\Gamma_4$  level of the  $T_d$  point group (we ignore the spin-orbit splitting of 0.07 eV).<sup>22</sup> These three levels correspond to the  $p_x$ ,  $p_y$ , and  $p_z$  orbitals of the *S* atoms. For growth on the (100) surface, the *x* and *y* direction remain equivalent, but differ from the *z* direction. Therefore, the triplet splits into a singlet and a doublet when the strain changes the point group from  $T_d$  to  $D_{2d}$ .

In closing, we would like to make a remark on the shear deformation potential, *b*, for CdS. One can estimate the deformation potential by the splitting between the light-

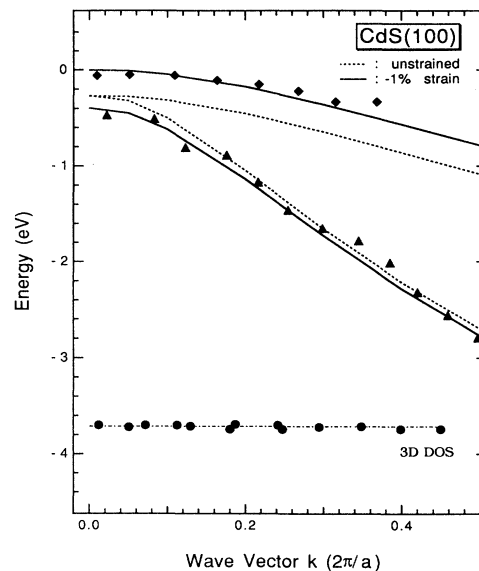


FIG. 3. Calculated (lines) and measured (points) dispersions of a CdS thin-film grown with a 1.0% in-plane biaxial strain. The transition energy of the data points was determined from the second derivative of the photoemission spectra as described in Ref. 20; the calculation is based on an EPM model.

and heavy-hole bands. The  $\Gamma$ -point theory predicts that in the absence of spin-orbit splitting the induced strain splitting is  $\delta E_{100} = 2b(\epsilon_1 - \epsilon_3)$ .<sup>11</sup> As discussed before, the biaxial in-plane stress leads to the perpendicular relaxation  $\epsilon_1 = -(2C_{12}/C_{11})\epsilon_3$ . Setting the spin-orbit splitting in CdS to zero and the strain to 1.0%, and taking the measured splitting to be 0.34 eV, one estimates the shear deformation potential  $b = 4.7$  eV which is somewhat higher than calculated values for similar zinc-blende semiconductors.<sup>10</sup>

## ACKNOWLEDGMENTS

The authors would like to thank the staff of the Synchrotron Radiation Center for their technical support, and M. Engelhardt for his assistance in the early stages of the experiment. D.W.N. is also indebted to S. Zollner for assistance with an EPM-based program at the Max Planck Institut für Festkörperforschung. D.W.N. would like to thank the Alexander von Humboldt Stiftung for partial financial support while the experiment was in progress.

\*Present address: National Renewable Energy Laboratory NREL, Golden, CO 80401-3393.

<sup>1</sup>C. Mailhot and D. L. Smith, CRC Crit. Rev. Solid State Mater. Sci. **16**, 131 (1990), and references therein.

<sup>2</sup>K. Shazad, D. J. Olego, C. G. Van de Walle, and D. A. Cammack, J. Lumin. **46**, 109 (1990), and references therein.

<sup>3</sup>Zong-Quan Gu, Ming-Fu Li, Jian-Qing Wang, and Bing-Sing Wang, Phys. Rev. B **41**, 8333 (1990).

<sup>4</sup>S. Ves, U. Schwarz, N. E. Christensen, K. Syassen, and M. Cardona, Phys. Rev. B **42**, 9113 (1990).

<sup>5</sup>R. People, Appl. Phys. Lett. **50**, 1604 (1987).

<sup>6</sup>M. J. Joyce and J. M. Dell, Phys. Rev. B **41**, 7749 (1990).

<sup>7</sup>R. People, Phys. Rev. B **32**, 1405 (1985).

<sup>8</sup>G. C. Osbourn, J. Vac. Sci. Technol. A **3**, 826 (1985).

<sup>9</sup>J. S. Nelson, S. R. Kurtz, L. R. Dawson, and J. A. Lott, Appl. Phys. Lett. **57**, 578 (1990).

<sup>10</sup>C. Van de Walle, Phys. Rev. B **39**, 1871 (1989).

<sup>11</sup>Manuel Cardona and Niels Christensen, Phys. Rev. B **35**, 6182 (1987).

<sup>12</sup>Khalid Shahzad, Diego J. Olego, and Chris G. Van de Walle, Phys. Rev. B **38**, 1417 (1988).

<sup>13</sup>J. Hwang, C. K. Shih, P. Pianetta, G. D. Kubiak, R. H. Stulen, L. R. Dawson, Y.-C. Pao, and J. S. Harris, Jr., Appl. Phys. Lett. **52**, 308 (1988).

<sup>14</sup>David W. Niles and Hartmut Höchst, Phys. Rev. B **41**, 12710 (1990).

<sup>15</sup>M. A. Engelhardt, D. W. Niles, and H. Höchst, J. Vac. Sci. Technol. A **8**, 1922 (1990).

<sup>16</sup>D. W. Niles and H. Höchst, Mater. Res. Soc. Symp. Proc. **208**, 243 (1991).

<sup>17</sup>K. Sinha, J. Menéndez, D. W. Niles, and H. Höchst, J. Vac. Sci. Technol. B **9**, 2202 (1991).

<sup>18</sup>J. W. Mathews and A. E. Blakeslee, J. Cryst. Growth **27**, 118 (1974).

<sup>19</sup>S. A. Chambers and V. A. Loebs, Phys. Rev. B **42**, 5109 (1990).

<sup>20</sup>David W. Niles and Hartmut Höchst, Phys. Rev. B **43**, 1492 (1991).

<sup>21</sup>R. D. Bringans, in *Angular-Resolved Photoemission*, edited by S. D. Kevan (Elsevier, New York, in press).

<sup>22</sup>M. Cardona, M. Weinstein, and G. A. Wolff, Phys. Rev. **140**, A633 (1965).

<sup>23</sup>K. J. Chang, S. Froyen, and M. L. Cohen, Phys. Rev. B **28**, 4736 (1983).